Heliyon 10 (2024) e33042

Contents lists available at ScienceDirect

Heliyon

journal homepage: www.cell.com/heliyon

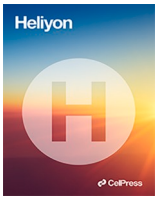

Research article

Development and characterization of a spark plasma device designed for medical and aesthetic applications

Mohammad Reza Lotfi [a], Mohammadreza Khani [a,*], Abootaleb Moradi [a], Elahe Razaghiha [a], Babak Shokri [a,b]

[a] Laser and Plasma Research Institute, Shahid Beheshti University, G.C., Evin, 1983963113, Tehran, Iran
[b] Department of Physics, Shahid Beheshti University, G.C. Evin, 19839-63113, Tehran, Iran

A B S T R A C T

Cold atmospheric plasma devices have shown high potential to be useful for different medical applications. In this study, it has been tried to develop and characterize a cold atmospheric spark plasma device that can be used safely as a tool for medical and aesthetic applications. The schematic of the device is presented in the paper, and the signals of each block are also tested. A special handpiece for this device is designed to make the device as safe as possible. The device's properties that can impose a risk to users' health have been under consideration. The device's electrical properties have been tested, and results show that the electrical current of the device is below the safety thresholds and can be used safely. The radiation power of the device also has been tested. It is shown that the time needed for the radiation power to reach the danger threshold is much longer than the treatment time. The device will not impose any risk regarding radiation from the UV spectrum. Optical emission spectroscopy is also used to investigate the neutral and charged species that are the by-products of electrical discharge. The presence of NO_x and OH locally in the discharge can be helpful for various medical applications. This paper presents one of the first studies conducted to investigate the engineering aspect and the immunometry of the spark plasma that can be used in medicine and other purposes.

1. Introduction

Atmospheric pressure plasma instruments have a rich history that extends beyond fifty years. Commencing in the latter half of the 20th century, specifically the late 1950s, the scientific community initiated investigations into atmospheric pressure plasma jets driven by arc mechanisms, with preliminary considerations for their market potential. Notably, Gabriel Gianinni emerged as an early innovator in this domain. His foresight in 1957 contemplated the application of these elevated-temperature plasma generators for thrust mechanisms [1,2] and cutting applications [3].

In the following decades, a comprehensive body of research was undertaken on these thermal plasma jets. These studies were distinguished by the examination of gas temperatures surpassing 10,000 K, aiming to elucidate the plasma-physical characteristics inherent to such high-temperature environments [4]. As the 1980s drew to a close, significant strides were taken to adapt processes involving low-pressure plasmas to those compatible with atmospheric pressure. This shift was aimed at obviating the necessity for expensive vacuum apparatuses. A notable advancement occurred in 1988 when Kurihara and colleagues successfully synthesized diamonds. To accomplish this feat, they employed a direct current (DC) plasma jet at heightened pressure levels, varying between 100 and 400 Torr [5].

In a development that transpired three years subsequent, the research conducted by Lu and associates culminated in the successful synthesis of diamonds under atmospheric pressure conditions. This was realized by integrating three direct current (DC) jets, with each

* Corresponding author.
E-mail address: khanimohammadreza@ymail.com (M. Khani).

https://doi.org/10.1016/j.heliyon.2024.e33042
Received 1 March 2024; Received in revised form 12 June 2024; Accepted 13 June 2024
Available online 13 June 2024

jet consuming approximately 12 kW. The process was facilitated by employing a gas mixture composed of argon and hydrogen [6]. A further significant instance that exemplifies the transition from low-pressure to atmospheric-pressure conditions is the utilization of a direct current (DC) plasma jet in the synthesis of fullerenes. This application was documented in the literature in the year 1992 [7]. Although these applications were pioneering and sporadic, it is important to note that thermal arc-based plasmas were principally utilized as sources of thermal energy, with a notable emphasis on their application in welding processes.

By the late 1990s, new concepts emerged for generating plasma jets at atmospheric pressure without relying on a transferred arc. These approaches included using pointed electrodes similar to corona discharges, employing dielectric materials to cover at least one electrode, reducing the discharge area through methods like micro-hollow cathode discharges, implementing discharge pulsing, and utilizing AC voltage signals [8–10]. Additionally, these alternative plasma generation methods brought about changes in plasma properties. Thermal plasma jets operating in Local Thermal Equilibrium (LTE) exhibited electron temperatures equal to that of heavy particles, resulting in high electron densities on the order of $10^{21}/m^3$ or even complete ionization [11].

Koinuma and colleagues pioneered the development of the initial HF cold atmospheric plasma (CAP) jet in 1992, as referenced in [12]. This plasma device features a cathode, a slender tungsten or stainless-steel needle electrode with a 1 mm diameter connected to an RF source operating at 13.56 MHz. This needle electrode is positioned within a quartz tube while the anode electrode is grounded. Different gases, often helium or argon, were combined depending on the intended application. The research group extensively documented various iterations and uses of this plasma jet in a series of publications [13–19].

In the year 2002, Stoffels et al. were instrumental in the introduction of a diminutive atmospheric plasma jet, aptly termed the "plasma needle" [20], followed by an improved version in 2004 [21]. In the previous design, the needle was housed within an enclosure, which required that samples be placed inside this enclosure for treatment. The revised design of the plasma needle features a metal filament of 0.3 mm in diameter, terminating in a finely honed point and encased within a Plexiglas cylinder. The entire length of the needle measures 8 cm, with 1.5 cm of the tip protruding beyond the Plexiglas sheath. Helium is selected as the gas of choice for its superior thermal conductivity properties. At the apex of the needle, a blend of helium and ambient air initiates a micro-discharge. Additionally, gases other than helium are utilized in this context [22]. The generation of a plasma glow, which is confined to a diameter of 2 mm, is achieved through the application of radio frequency (RF) power. This RF power operates at a frequency of 13.05 MHz and varies in intensity from 10 mW to several watts. The diminutive scale of the microplasma renders it particularly apt for targeted treatments in confined spaces, exemplified by dental procedures [23–28].

In 2012, another configuration of CAPs was introduced by Lu and colleagues [29] in which a needle is used as a high-voltage electrode. According to Paschen's law, the plasma is created when the counter electrode is close enough so that the electrical discharge can occur. This configuration of CAP is now known as spark plasma and has found its applications in medical and aesthetic applications.

In 2012, Scarano and colleagues [30] conducted the first experiment to prove spark plasma's applicability in rejuvenation and improving signs of aging. This group of researchers also proved the applicability of this configuration of plasma devices in the treatment of xanthelasma [31]. In 2014, Tsioumas and colleagues conducted the first experiment for the application of spark plasma in non-invasive blepharoplasty. Also, they compared the results of this method with those of traditional blepharoplasty surgery [32–34]. In 2015, Tsioumas and colleagues presented the result of their histological study, which showed that treatment with spark plasma could cause an increase in the production of collagen and contraction of elastic fibers [35]. According to histological investigation findings, spark plasma can vaporize the outer skin layer (epidermis) without traversing the basal layer. Research has demonstrated that the depth to which spark plasma penetrates the skin remains within the range of 0.1 mm [36–38]. Spark plasma has the potential to induce the contraction of elastic fibers and generate type III collagen, all while avoiding undesirable skin damage. Furthermore, examinations utilizing confocal microscopes reveal the efficacy of spark plasma in rejuvenating collagen structures that have undergone alterations due to aging [39,40]. The utilization of spark discharges is rapidly gaining prominence as a technology for skin rejuvenation and the treatment of various skin conditions, including skin moles, solar lentigo, seborrheic keratosis, active acne, post-acne scars, and

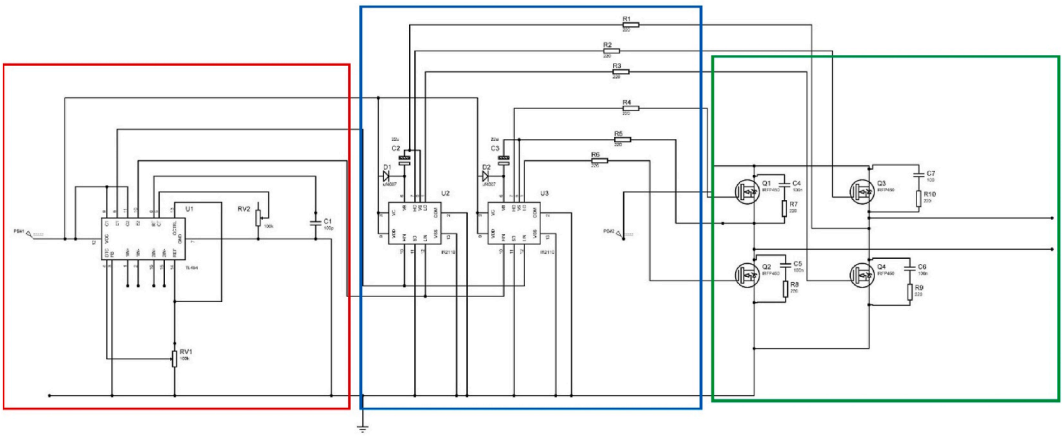

Fig. 1. Frequency and duty cycle controller circuit schematic. The voltage booster and internal power supply circuits are not shown for brevity.

even specific abnormalities like Darwin's tubercle [41–45].

Various studies investigate the possibility of using different plasma configurations for clinical and therapeutic applications [46–49]. In this paper, efforts have been made to develop and characterize a spark plasma device's electrical and mechanical parts and compare the results with international standards.

2. Experimental setup

In order to develop a suitable power supply for spark plasma that can be used in medical applications, there has been a need to design a power supply with adjustable frequency and duty cycle, which also exploits high voltages to be able to cause electrical breakdown between the electrode and the target. In order to achieve this goal, the power supply will be an aggregation of three main blocks, as shown in the circuit schematic (Fig. 1).

The first block is the "control block" (red box), which includes 2 main parts: a 12V power supply that can provide 3 amps of electrical current and is used to run a TL494 IC for PWM modulation. RV1 and RV2 are variable resistors with a range of 0-100k ohm. According to the schematic, RV1 is connected to PIN#4, 13, and 14. It can adjust the duty cycle, and RV2 is connected to PIN#5 and adjust the frequency. Regarding the values of RV2 and C1, the device's frequency can rise up to 200 kHz. PIN#9 and 10 are the output signals of the IC and are connected to the HIN and LIN PINs of the MOSFET drivers in the next block.

The second block is the "driver block" (blue box), which includes two MOSFET drivers IR2110 and is used to run the MOSFETs in the subsequent (3rd) block. According to the datasheet, the connections and components used in this block have been chosen. R1-R6 are 220-Ω 2-W resistors that decrease the value of the electrical current that flows through the circuit.

The third block is the "power block" (green box) and includes a power supply with variable voltage (PS#2); this power supply can provide a DC voltage in a range of 39–49V and an electrical current up to 4 amps. The complete bridge circuit in this block consists of 4 IRFP 450 MOSFETs. The drain and the source of each mosfet are connected using so-called "snubbers." A snubber is a device (a resistor and a capacitor connected in series) used to limit (or suppress) voltage spikes in electrical systems. In an electrical system with a sudden interruption in the flow of electricity, there may be a corresponding significant increase in voltage across the device.

After designing the circuit that enables one to adjust the device's voltage, duty cycle, and frequency, the output must be sent to a high-voltage, high-frequency transformer to provide the required voltage. According to (Fig. 1), the output signals are taken from the connection between adjacent MOSFETs' source and drain PINs. The output signals are connected to a handmade/non-commercial transformer with a primary-to-secondary ratio of 1:50 with a ferrite core. In spark plasma devices, only one high-voltage electrode is needed; in order to adjust the configuration following the desired result, one end of the wire in the output of the transformer will be connected to the ground, and the other end will be connected to the special handpiece designed for the spark plasma application (Fig. 2a and b).

The handpiece is ergonomic and made explicitly for spark plasma applications. The main body of the handpiece is 20 cm and is made and filled with PTFE. This electrical insulator will reduce the risk of electrical shock and is covered with a layer of aluminum. The handpiece has a uniquely designed connector that can be used as a place for needle electrodes. Any disposable dental needle can be used as the electrode to help users follow hygienic protocols. To adhere to the prescribed norms, electrodes were constituted of AVA stainless steel dental needles (manufactured by AVA pezeshk Co., Iran, bearing the Standard license number: 91943955).

3. Results

The electrical measurements have been taken on this device and compared with standards to ensure that it can be used safely in medical applications. The electrical measurements have been done on every block using a digital oscilloscope (Tektronix DPO 3012). In this apparatus, due to the utilization of a substantial potential difference for electrical breakdown, a high-voltage probe (Tekterorix, P6015A, with a ratio of 1:1000) is employed to ascertain the voltage across the high-voltage transformer.

As described in the previous section, the "control block" uses an IC for pulse width modulation. This block is connected to a 12V DC power supply, and the output signals are taken from PIN#9 and #10. The test shows that every PIN can provide a square signal, and its

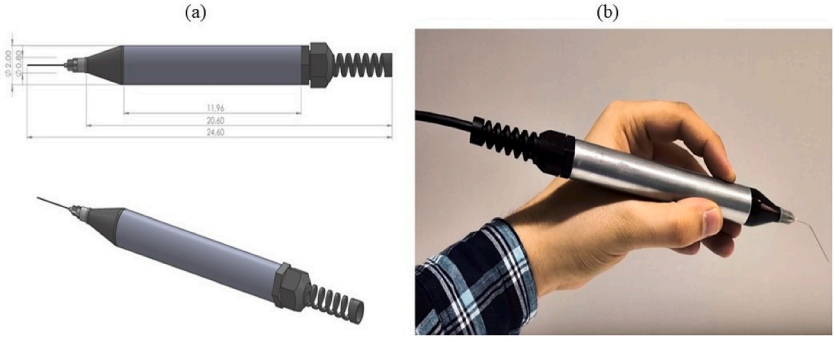

Fig. 2. The design (a) and production (b) sample of the handpiece for the spark plasma device.

duty cycle can change from 0 to 50 %. The signals have an amplitude of 12V, and their frequency can vary up to 200 kHz (Fig. 3 a&b).

The output signals of the first block are connected to the gate driver ICs in the "driver block." This block uses the same power supply of 12V DC and is used to run the MOSFETs in the next block. Each driver has three output signals (High-side, Low-side, and supply voltage) and is connected to the three PINs of MOSFETs according to (Fig. 1). The output signal of the IR2110 ICs, just like the previous case, is a square signal with an amplitude of 12V and a frequency up to 200 kHz (Fig. 4 a&b).

The full bridge circuit in the "power block" will provide a bipolar square signal with an adjustable frequency and duty cycle. Adjacent MOSFETs will provide the positive and negative peaks (according to (Fig. 5)), which, when combined, will result in a bipolar square signal.

According to (Fig. 5), positive and negative peaks will turn on and off in specific periods. If the red and blue graphs in (Fig. 5) combine, it can be seen that the result will be a bipolar signal. The output of the bipolar signal is taken from the connection between the drain and the source of adjacent MOSFETs and is sent to the transformer (Fig. 6a). The output signal is connected to a 1:50 transformer, which will increase the voltage. The output peak-to-peak voltage corresponding to the highest duty cycle is 4.621 kV (Fig. 6b) and has a sinusoidal waveform.

In many articles, the resistance of human skin has been investigated. In these studies, it has been shown that the resistance of human skin has values between 1 and 100 kilohms depending on the examined area [50]. For this reason, a resistance that has a negligible value compared to the resistance of the human skin has been used to calculate the amount of electric current resulting from the electric discharge. This research, a 10-Ω resistor is used to check the electric current resulting from the electric discharge, which is placed in the circuit according to the (Fig. 7a). Also, many studies have been conducted to achieve a suitable equivalent circuit for simulating the electrical properties of human skin [51]. In this study, a Japanese leakage current circuit (Fig. 7b), mentioned in the IEC 60601-1 standard [52] as a standard circuit, has been used to investigate the value of current passing through the human skin.

The findings from this study indicate that the peak electrical current of the discharge, as delineated in the schematic of Fig. 7(a), registers at 2.6 mA, a value corroborated by Fig. 8(a). The root mean square (rms) of this electrical current is documented at 1.26 mA. Furthermore, the maximum patient leakage current detected by the device is significantly lower, recorded at 0.3 mA as depicted in Fig. 8(b), with an rms value of 0.1 mA. This level is deemed safe in accordance with the IEC60601-1 standard. The ET 213:2007 standard posits that an electrical current of 5 mA sustained for 5 s may induce involuntary muscle contractions. Nevertheless, such electrical currents present no peril to the vitality of living tissues or the overall health of the organism.

The discharge power was ascertained utilizing a capacitor with a capacitance of. The computation of the device's discharge power is derived from the Q-V diagram's enclosed loop, as illustrated in (Fig. 9). By calculating the energy per discharge cycle and then multiplying this energy by the cycle's frequency, the power of the discharge is deduced [53]. The power of the discharge corresponding to the highest duty cycle is 1.2W. In a similar research context investigating the electrical characteristics of a different configuration of cold atmospheric plasma (plasma jet), Nastuta and colleagues focused their attention on both helium and argon plasma jets. Regarding the argon plasma jet, the discharge current exhibited a range of fluctuations, spanning from 4.2 to 4.5 mA.

In contrast, the helium discharge registered a consistent 2 mA. Regarding power measurements, the recorded values for the argon plasma jet ranged between 0.7 and 1W. In contrast, the helium plasma jet's power fluctuated between 0.4 and 0.9W [54].

The radiated power of the apparatus is quantified employing a Nova IIP/N7Z01550 power meter (Ophir Photonics Group). This instrument gauges the emitted radiation from the device when in proximity to the target surface, specifically at intervals of 5 cm and 10 cm. To mitigate electromagnetic interference (EMI), the assessments were conducted within a sequestered, dimly-lit clean chamber. An enclosure fashioned from cardboard was utilized to insulate the measurements from external influences, ensuring that illumination from the power meter's display did not perturb the data acquisition process.

In alignment with the guidelines set forth by the German Dermatological Society, it is advised that the commencement doses for broadband UV-B (spanning 280–320 nm) should range from 20 to 60 mJ/cm^2, contingent upon the individual's skin type. Conversely, for narrow-spectrum UV-B (at 311 nm), the recommended starting doses are markedly greater, lying between 200 and 600 mJ/cm^2 [55]. In accordance with the directives of the International Commission on Non-Ionizing Radiation Protection (ICNIRP), the guidelines stipulate that for the most delicate, non-pathological skin types, the limit for non-therapeutic and non-elective ultraviolet (UV) exposure within the spectral range of 180–400 nm should not surpass 30 J/m^2 or equivalently, 3 mJ/cm^2. These thresholds are

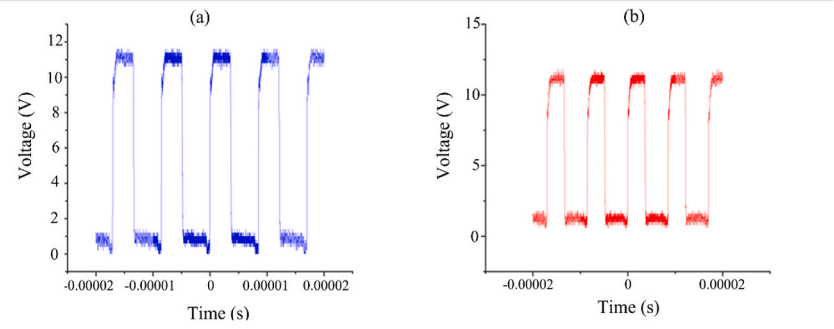

Fig. 3. The signals of the control block with frequency of 200 kHz and duty cycle of 50 %. (a) represents the signal from PIN#9 and (b) is the signal from PIN#10.

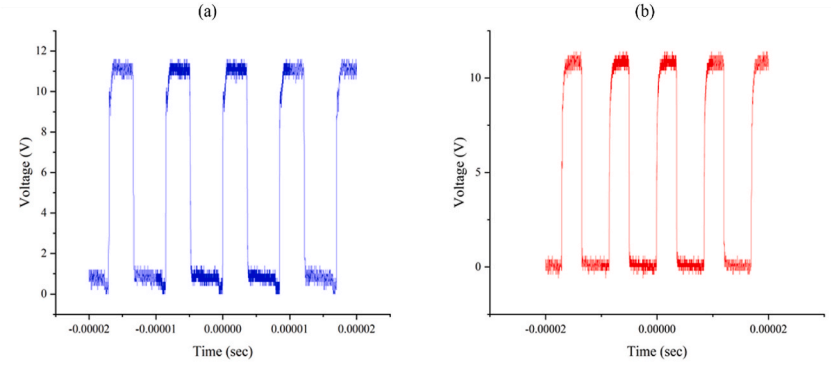

Fig. 4. The output signals of the driver block with frequency of 200 kHz. (a) represents the output signal of High-side PIN and (b) represents the output signal of the Low-side PIN.

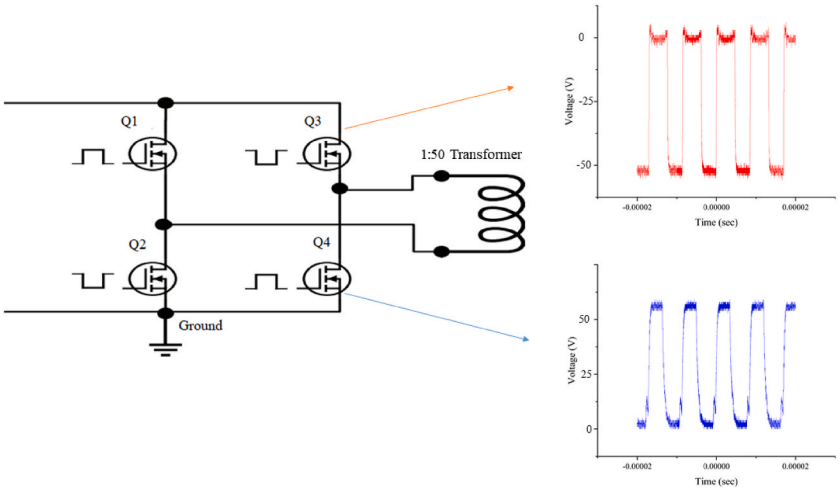

Fig. 5. The view of connecting the output signals of the full bridge circuit to the voltage booster transformer and the shape of the positive peak and negative valley signals. As it can be seen the red graph represents the negative peak of the voltage varying from 0 to −50 V and the blue graph represents the positive peak varying from 0 to 50 V. Combination of these two signals which is a voltage signal varying from −50 to 50 V will be connected to the high voltage transformer. (For interpretation of the references to colour in this figure legend, the reader is referred to the Web version of this article.)

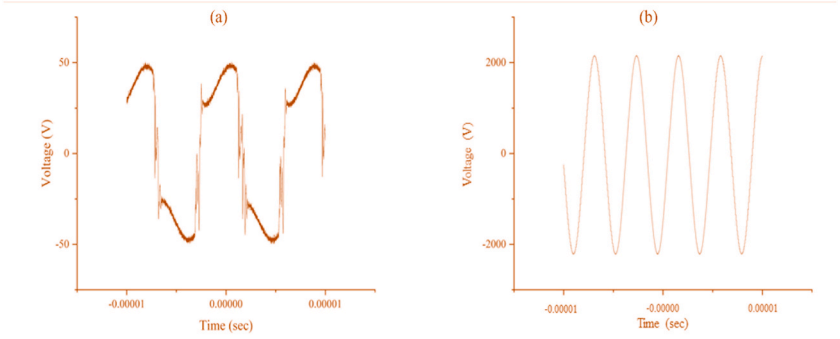

Fig. 6. The shape and amplitude of the bipolar signal before and after increasing the voltage can be seen. (a) The signal's shape before the voltage increase results from combining the positive and negative poles at the output of MOSFETs which was show in Fig. 5. (b) represents the voltage signal after the voltage boost.

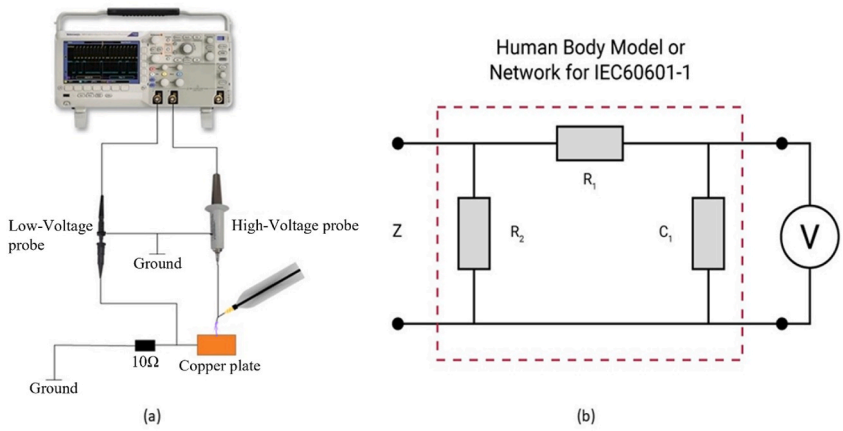

Fig. 7. Schematic of the circuit designed to measure the electric current resulting from the discharge (a) and the equivalent circuit of the human body (b) to check the electrical safety of the device.

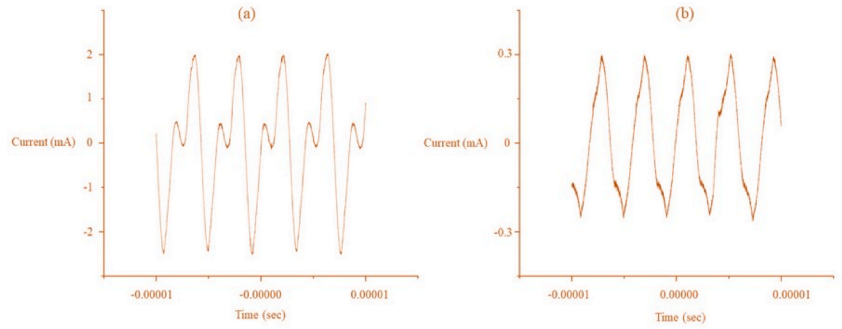

Fig. 8. (a) the current signal of the spark discharge measured according to the circuit show in Fig. 7(a). (b) the signal of leakage current measured according to the standard circuit shown in Fig. 7(b).

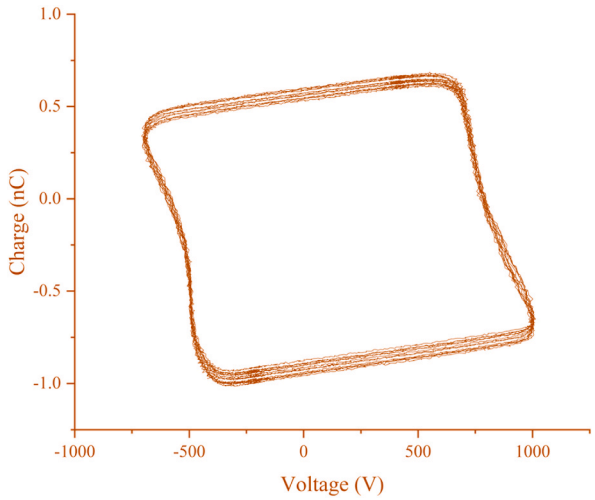

Fig. 9. The Charge-Voltage diagram of the plasma which is used to calculate the power of the discharge.

established to safeguard sensitive skin against the potential risks associated with UV radiation [56].

The UV emission dose of the device, when set to its maximum power and duty cycle, was measured at 7.86×10^{-4} W/m^2 in proximity to the discharge. This measurement is significantly lower by an order of magnitude compared to the values documented for

the commercially distributed SteriPlas plasma torches (produced by Adtec Europe Ltd, London, UK) [57]. The data suggests that a continuous discharge duration of **635** min meets the benchmark set by the ICNIRP guidelines. At a separation of 5 and 10 cm from the discharge source, the UV radiation levels were undetectable. It is particularly noteworthy that the UV radiation emitted could lead to more adverse effects, such as the creation of crusts on exposed tissue. Consequently, the emission levels of UV radiation warrant careful consideration during the development phase of new devices or applications, to mitigate potential harmful effects.

The investigation employed an optical emission spectroscopy apparatus (OES; Avaspec3648USB2) to analyze the assortment of active and reactive entities within cold plasma, as well as to scrutinize the chemical and physical attributes of spark plasmas. The spectral data captured by the OES spanned from 200 to 450 nm along the axis of the plasma. The spectroscopic procedure was executed in a darkened chamber in direct proximity to the discharge event, with calibration to a zero baseline conducted at the precise site of measurement. The integration period was established at 500 ms, which facilitated an automatic 10-fold averaging by the device's computational software (avasoft).

Optical emission spectroscopy (OES) offers considerable benefits in the realm of materials processing, owing to its capacity to establish correlations between plasma characteristics and material properties. This technique is notably straightforward when the available instrumentation is conducive to its application. As a diagnostic tool for plasma analysis, spectroscopic methods are particularly resistant to interference, focusing on the examination of radiation—whether emitted, absorbed, or scattered—to ascertain the parameters of the plasma [58,59]. The application of optical emission spectroscopy (OES) on the spark plasma provided a deeper insight into the chemical composition of these discharges. The OES findings revealed the detection of various species, including OH at 309 nm, NO within the 200–250 nm range, and N2/N2+ at 297, 315, 337, 358, 375.4, and 380 nm [60,61]. These results are detailed further in (Fig. 10). It is important to highlight that the spectral evidence of NO is discernible only under conditions of high power and increased duty cycles. In line with expectations, there is a direct correlation between the peak intensities and the escalation in both power and duty cycle.

4. Conclusion

Design and implementation of an adjustable cold atmospheric spark plasma device is done. Investigations indicate that this particular structure and combination of electrical and mechanical instruments can result in a suitable and safe spark plasma device for medical and aesthetic applications.

The electrical results indicate that the current value is under the safety threshold. Regarding the electrical shock, this device can perform safely. The breakdown voltage might be considered dangerous, but in this case, the device can be used without any imposed risk to users' health because of the high frequency.

The radiation power is much below the safety threshold as well. The continuous discharge for 635 min was observed to radiate enough UV to be considered dangerous according to the ICNIRP standard. The OES indicates the presence of chemical compounds that can be helpful for the overall health of the skin. For example, NOx is one of the essential agents for cell signaling that increases the wound's healing rate. The presence of OH in the OES spectroscopy also can indicate that in lower discharge durations that cause less or no tissue damage (which can be achieved by reducing the duty cycle), this device can be used as a tool for disinfection of wounds as

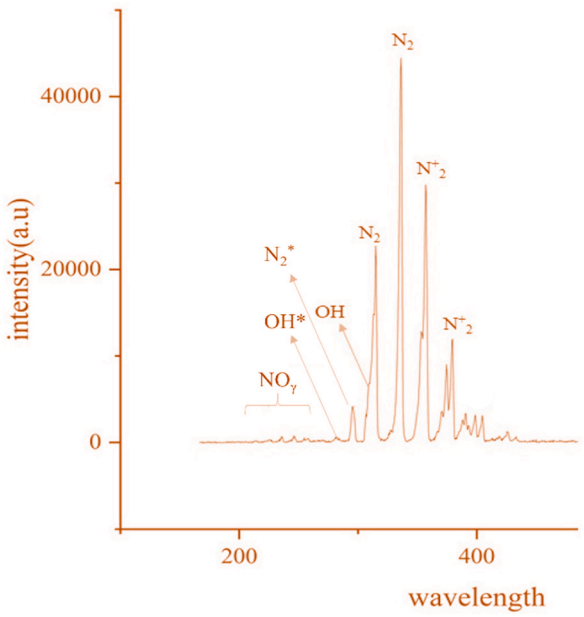

Fig. 10. The graph obtained from optical emission spectroscopy indicates the presence of active species that can expand the field of device applications.

well as rejuvenation.

Such features of the proposed design bring advantages to high-voltage power supplies but can also facilitate the commercial development of plasma system applications.

Data availability

The data that support the findings of this study are available on request from the corresponding author, [M.K].

CRediT authorship contribution statement

Mohammad Reza Lotfi: Writing – review & editing, Writing – original draft, Visualization, Validation, Software, Resources, Methodology, Investigation, Formal analysis, Data curation, Conceptualization. **Mohammadreza Khani:** Writing – review & editing, Writing – original draft, Visualization, Validation, Supervision, Resources, Project administration, Methodology, Investigation, Funding acquisition, Formal analysis, Data curation, Conceptualization. **Abootaleb Moradi:** Writing – review & editing, Methodology, Investigation, Data curation. **Elahe Razaqiha:** Writing – review & editing, Software, Methodology, Investigation, Data curation, Conceptualization. **Babak Shokri:** Writing – review & editing, Validation, Supervision, Project administration, Conceptualization.

Declaration of competing interest

The authors declare that they have no known competing financial interests or personal relationships that could have appeared to influence the work reported in this paper.

References

[1] G.M. Giannini, The plasma jet, Sci. Am. 197 (2) (1957) 80–90.
[2] M. Andrenucci, Giannini, Ducati and the dawn of MPD propulsion, in: SP2010–1855072, 2010.
[3] G. Gianinni, A. Ducati, Plasma Steam Apparatus and Methods, 1960. US2922869 AUSP Office Go to reference in article.
[4] H. Conrads, M. Schmidt, Plasma generation and plasma sources, Plasma Sources Sci. Technol. 9 (4) (2000) 441.
[5] K. Kurihara, et al., High rate synthesis of diamond by dc plasma jet chemical vapor deposition, Appl. Phys. Lett. 52 (6) (1988) 437–438.
[6] Z. Lu, et al., Diamond synthesis by DC thermal plasma CVD at 1 atm, Plasma Chem. Plasma Process. 11 (1991) 387–394.
[7] K.i. Yoshie, et al., Novel method for C60 synthesis: a thermal plasma at atmospheric pressure, Appl. Phys. Lett. 61 (23) (1992) 2782–2783.
[8] A. Schutze, et al., The atmospheric-pressure plasma jet: a review and comparison to other plasma sources, IEEE Trans. Plasma Sci. 26 (6) (1998) 1685–1694.
[9] K. Schoenbach, et al., Microhollow cathode discharges, J. Vac. Sci. Technol. A: Vacuum, Surfaces, and Films 21 (4) (2003) 1260–1265.
[10] J.F. Kolb, et al., Cold atmospheric pressure air plasma jet for medical applications, Appl. Phys. Lett. 92 (24) (2008).
[11] C. Tendero, et al., Atmospheric pressure plasmas: a review, Spectrochim. Acta B Atom Spectrosc. 61 (1) (2006) 2–30.
[12] H. Koinuma, H. Ohkubo, T. Hashimoto, K. Inomata, T. Shiraishi, A. Miyanaga, S. Hayashi, Development and application of a microbeam plasma generator, Appl. Phys. Lett. 60 (7) (1992) 816–817.
[13] K. Inomata, H. Ha, K.A. Chaudhary, H. Koinuma, Open air deposition of SiO2 film from a cold plasma torch of tetramethoxysilane-H2-Ar system, Appl. Phys. Lett. 64 (1994) 46.
[14] H. Ha, K. Inomata, H. Koinuma, Plasma chemical vapor deposition of SiO2 on air-exposed surfaces by cold plasma torch, J. Electrochem. Soc. 142 (8) (1995) 2726–2730.
[15] K. Inomata, H. Koinuma, Y. Oikawa, T. Shiraishi, Open air photoresist ashing by a cold plasma torch: catalytic effect of cathode material, Appl. Phys. Lett. 66 (1995) 2188.
[16] H. Ha, M. Yoshimoto, H. Koinuma, B.K. Moon, H. Ishiwara, Open air plasma chemical vapor deposition of highly dielectric amorphous TiO2 films, Appl. Phys. Lett. 68 (1996) 2965.
[17] H. Ha, B.K. Moon, T. Horiuchi, T. Inushima, H. Ishiwara, H. Koinuma, Structure and electric properties of TiO2 films prepared by cold plasma torch under atmospheric pressure, Mater Sci Eng B41 (1) (1996) 143–147.
[18] K. Inomata, N. Aoki, H. Koinuma, Jpn. J. Appl. Phys. 33 (1994) 197.
[19] B. Lee, Y. Kusano, N. Kato, K. Naito, T. Horiuchi, H. Koinuma, Oxygen plasma treatment of rubber surface by the atmospheric pressure cold plasma torch, Jpn. J. Appl. Phys. 36 (5A) (1997) 2888–2891.
[20] E. Stoffels, A.J. Flikweert, W.W. Stoffels, G.M.W. Kroesen, Plasma needle: a non–destructive atmospheric plasma source for fine surface treatment of (bio) materials, Plasma Sources Sci. Technol. 4 (2002) 383–388.
[21] I.E. Kieft, Laan Epvd, E. Stoffels, Electrical and optical characterization of the plasma needle, New J. Phys. 6 (2004) 149.
[22] S.-Z. Li, W.-T. Huang, J. Zhang, D. Wang, Optical diagnosis of an argon/oxygen needle plasma generated at atmospheric pressure, Appl. Phys. Lett. 94 (2009) 111501.
[23] S. Govil, V. Gupta, S. Pradhan, Plasma needle: the future of dentistry, Indian J. Basic Appl. Med. Res. 1 (2) (2012) 143–147.
[24] C. Jiang, M.A. Gundersen, C. Schaudinn, P. Webster, D.E. Jaramillo, P.P. Sedghizadeh, J.W. Costerton, An atmospheric pressure non-thermal plasma needle for endodontic biofilm disinfection, in: IEEE Int Confer Plasma Sci – ICOPS, 2011, p. 1, 1.
[25] LJ Van den Bedem, RE Sladek, M Steinbuch, E Stoffels Adamowicz, Plasma treatment of S. mutans biofilms cultured in a simulated dental cavity model. Eindhoven, the Netherlands: XXVIIth ICPIG 18 (2005 Jul).
[26] C. Schaudinn, D. Jaramillo, M.O. Freire, P.P. Sedghizadeh, A. Nguyen, P. Webster, J.W. Costerton, C. Jiang, Evaluation of a nonthermal plasma needle to eliminate ex vivo biofilms in root canals of extracted human teeth, Int. Endod. J. 46 (10) (2013) 1–8.
[27] R.E.J. Sladek, S.K. Filoche, C.H. Sissons, E. Stoffels, Treatment of Streptococcus mutans biofilms with a nonthermal atmospheric plasma, Lett. Appl. Microbiol. 45 (3) (2007) 318–323.
[28] R.E.J. Sladek, T.A. Baede, E. Stoffels, Plasma-needle treatment of substrates with respect to wettability and growth of Escherichia coli and Streptococcus mutans, IEEE T Plasma Sci 34 (2006) 1325–1330.
[29] X. Lu, M. Laroussi, V. Puech, On atmospheric-pressure non-equilibrium plasma jets and plasma bullets, Plasma Sources Sci. Technol. 21 (3) (2012) 034005.
[30] A. Scarano, et al., Treatment of perioral rhytides with voltaic arc dermoabrasion, Eur. J. Inflamm. 10 (1 Supplement 2) (2012) 25–29.
[31] A. Scarano, et al., Treatment of xanthelasma palpebrarum with voltaic arc dermoabrasion, Int. J. Immunopathol. Pharmacol. 1 (3) (2012) 17–22.
[32] Tsioumas G. Sotiris, Georgiadis Nikolaos, Georgiadou Irini, Plexr: the revolution in blepharoplasty, ISSN: 2360-9516, Pinnacle Medicine & Medical Sciences 1 (5) (2014) 423–427. Article ID pmms_160.

[33] Tsioumas G. Sotiris, Georgiadou Irini, Ntountas Ioannis, Non-invasive upper blepharoplasty in relation to surgical blepharoplasty, ISSN: 2360-9516, Pinnacle Medicine & Medical Sciences 1 (5) (2014) 436–440, 2014, Article ID pmms_163.
[34] M. Lotfi, M. Khani, B. Shokri, A review of cold atmospheric plasma applications in dermatology and aesthetics, Plasma Med. 13 (1) (2023).
[35] Tsioumas G. Sotiris, Vlachodimitropoulos Dimitris, Goutas Nikolaos, Clinical and histological presentation after plexr application, needle shaping (Vibrance) and OFF, ISSN: 2360-9516, Pinnacle Medicine & Medical Sciences 2 (3) (2015) 522–530, 2014, Article ID pmms_178.
[36] G. Tsioumas, N. Georgiadis, I. Georgiadou, The gas ionization by plasma technology for non-invasive techniques in oculoplastic, JOJ Ophthal 2 (2) (2017) 555–584.
[37] T.G. Sotiris, G. Nikolaos, G. Irini, New treatment with plasma exeresis for non-surgical blepharoplasty, EC Ophthalmology 5 (4) (2017) 156–159.
[38] T. Sotirios, S. Nantia, Non invasive blepharoplasty with plasma exeresis (Plexr) pre/post treatments, J Aesthetic Reconstr Surg 4 (1) (2018) 1–4.
[39] Georgia Gloustianou, Maria Sifaki, Sotiris G. Tsioumas, Dr Vlachodimitropoulos, Antonio Scarano, Presentation of old and new histological results after plasma exercises (plexr) application (regeneration of the skin tissue with collagen III), ISSN: 2360-9516, Pinnacle Medicine & Medical Sciences 3 (3) (2016) 983–990, 2016, Article ID pmms_241.
[40] E. Rossi, F. Farnetani, M. Trakatelli, S. Ciardo, G. Pellacani, Clinical and confocal microscopy study of plasma exeresis for nonsurgical blepharoplasty of the upper eyelid: a pilot study, Dermatol. Surg. 44 (2) (2018 Feb 1) 283–290.
[41] A. Baroni, Long-wave plasma radiofrequency ablation for treatment of xanthelasma palpebrarum, J. Cosmet. Dermatol. 18 (1) (2019) 121–123.
[42] I. Verner, H.P. Naveh, S. Cotofana, A novel ablative radiofrequency microplasma nonsurgical blepharoplasty for dermatochalasis, Dermatol. Ther. 33 (6) (2020) e14002.
[43] A. Scarano, F. Carinci, F. Festa, V. Candotto, R. Amore, F. Lorusso, Periauricular wrinkles removed with voltaic arc dermabrasion (Atmospheric Plasma technique), J. Cosmet. Dermatol. 19 (7) (2020 Jul) 1709–1714.
[44] E. Rossi, F. Farnetani, G. Pellacani, Applications of plasma exeresis in dermatology, Hi-Tech Dermo 2 (2016) 17–22.
[45] R. Valeriani, G. Firmani, M. Valeriani, Correction of Darwin's tubercle with plasma exeresis, Plastic and Reconstructive Surgery Global Open 10 (10) (2022).
[46] F. do Nascimento, A. da Graça Sampaio, N.V. Milhan, A.V. Gontijo, P. Mattern, T. Gerling, E. Robert, C.Y. Koga-Ito, K.G. Kostov, A low cost, flexible atmospheric pressure plasma jet device with good antimicrobial efficiency, IEEE Trans. Radiat. Plasma Med. Sci. 8 (3) (2024) 307–322.
[47] A.V. Nastuta, T. Gerling, Cold atmospheric pressure plasma jet operated in Ar and He: from basic plasma properties to vacuum ultraviolet, electric field and safety thresholds measurements in plasma medicine, Appl. Sci. 12 (2) (2022 Jan 10) 644.
[48] K.D. Weltmann, E. Kindel, R. Brandenburg, C. Meyer, R. Bussiahn, C. Wilke, T. Von Woedtke, Atmospheric pressure plasma jet for medical therapy: plasma parameters and risk estimation, Contrib. Plasma Phys. 49 (2009 Oct 15).
[49] M. Xaubet, J.S. Baudler, T. Gerling, L. Giuliani, F. Minotti, D. Grondona, T. Von Woedtke, K.D. Weltmann, Design optimization of an air atmospheric pressure plasma-jet device intended for medical use, Plasma Process. Polym. 15 (8) (2018 Aug) 1700211.
[50] R.M. Fish, L.A. Geddes, Conduction of electrical current to and through the human body: a review, Eplasty 9 (2009).
[51] A. Stancampiano, T.H. Chung, S. Dozias, J.M. Pouvesle, L.M. Mir, E. Robert, Mimicking of human body electrical characteristic for easier translation of plasma biomedical studies to clinical applications, IEEE transactions on radiation and plasma medical sciences 4 (3) (2019 Aug 21) 335–342.
[52] K-D Weltmann, Th. von Woedtke, Basic requirements for plasma sources in medicine, *The European Physical Journal - Applied Physics* 55 (1) (2011) 13807, https://doi.org/10.1051/epjap/2011100452DIN SPEC 91315:2014-06.
[53] M. Kettlitz, et al., On the spatio-temporal development of pulsed barrier discharges: influence of duty cycle variation, J. Phys. Appl. Phys. 45 (24) (2012) 245201.
[54] A.V. Nastuta, T. Gerling, Cold atmospheric pressure plasma jet operated in Ar and He: from basic plasma properties to vacuum ultraviolet, electric field and safety thresholds measurements in plasma medicine, Appl. Sci. 12 (2) (2022) 644.
[55] Empfehlungen zur Phototherapie und Photochemotherapie. 2002/2007, Deutsche Dermatologische Gesellschaft (DDG).
[56] I.C.o.N.-I.R. Protection, Guidelines on limits of exposure to ultraviolet radiation of wavelengths between 180 nm and 400 nm (incoherent optical radiation), Health Phys. 87 (2) (2004) 171–186.
[57] A. Bennett, et al., Characterisation of a cold atmospheric pressure plasma torch for medical applications: demonstration of device safety, Appl. Sci. 11 (24) (2021) 11864.
[58] D. Devia, L. Rodriguez-Restrepo, E.R. Parra, Methods employed in optical emission spectroscopy analysis: a review, Ingeniería y ciencia 11 (21) (2015) 239–267.
[59] J. Coburn, M. Chen, Optical emission spectroscopy of reactive plasmas: a method for correlating emission intensities to reactive particle density, J. Appl. Phys. 51 (6) (1980) 3134–3136.
[60] T. Darny, J.M. Pouvesle, V. Puech, C. Douat, S. Dozias, E. Robert, Analysis of conductive target influence in plasma jet experiments through helium metastable and electric field measurements, Plasma Sources Sci. Technol. 26 (4) (2017 Mar 10) 045008.
[61] J.L. Hueso, V.J. Rico, Á. Yanguas-Gil, J. Cotrino, A.R. González-Elipe, Optical emission spectroscopic evaluation of different microwave plasma discharges and its potential application for sterilization processes, in: Plasma for Bio-Decontamination, Medicine and Food Security, Springer, Netherlands, 2012, pp. 121–132.